



# Multimodal Functional Imaging in Tumor-induced Osteomalacia: $^{68}\text{Ga}$ -DOTATATE, $^{18}\text{F}$ -FDG, and $^{68}\text{Ga}$ -FAPI PET/CT Findings

Tümör Kaynaklı Osteomalazide Multimodal Fonksiyonel Görüntüleme:  $^{68}\text{Ga}$ -DOTATATE,  $^{18}\text{F}$ -FDG ve  $^{68}\text{Ga}$ -FAPI PET/BT Bulguları

✉ Zehranur Tosunoğlu<sup>1</sup>, ✉ Utku Erdem Soyaltın<sup>2</sup>, ✉ İpek Öztürk<sup>3</sup>, ✉ Meryem Kaya<sup>3</sup>, ✉ Burcu Esen Akkaş<sup>3</sup>, ✉ Esra Arslan<sup>1</sup>

<sup>1</sup>University of Health Sciences Türkiye, İstanbul Training and Research Hospital, Clinic of Nuclear Medicine, İstanbul, Türkiye

<sup>2</sup>Ege University Faculty of Medicine, Department of Internal Medicine, Division of Endocrinology and Metabolism, İzmir, Türkiye

<sup>3</sup>University of Health Sciences Türkiye, Başakşehir Çam and Sakura City Hospital, Clinic of Nuclear Medicine, İstanbul, Türkiye

## Abstract

Tumor-induced osteomalacia, resulting from tumoral overproduction of fibroblast growth factor 23, is a rare paraneoplastic syndrome clinically characterized by muscle weakness, bone pain, and pathological fractures. Fewer than 1,000 cases have been reported in the literature. Laboratory findings typically include hypophosphatemia, normal or decreased levels of 1.25-dihydroxy vitamin D, and normal or elevated levels of FGF23. Functional imaging methods, particularly somatostatin receptor imaging, play an important role in the localization of the tumor. In this case of tumor-induced osteomalacia, we presented the findings from gallium-68 ( $^{68}\text{Ga}$ )-DOTATATE,  $^{68}\text{Ga}$ -fibroblast, and  $^{18}\text{F}$ -fluorodeoxyglucose positron emission tomography imaging modalities used for tumor localization.

**Keywords:** Tumor-induced osteomalacia, phosphaturic mesenchymal tumors,  $^{68}\text{Ga}$ -DOTATATE PET/CT,  $^{68}\text{Ga}$ -FAPI PET/CT,  $^{18}\text{F}$ -FDG PET/CT

## Öz

Fibroblast büyüme faktörü 23'ün tümöral üretimine bağlı gelişen tümör kaynaklı osteomalazi, kas güçsüzlüğü, kemik ağrısı ve patolojik kırıklarla seyreden, nadir görülen bir paraneoplastik sendromdur. Literatürde bildirilen olgu sayısı 1000'in altındadır. Laboratuvar bulguları, hipofosfatemi, normal veya düşük düzeyde 1.25-dihidroksi vitamin D ve normal ya da artmış FGF23 düzeyleri ile karakterizedir. Tümörün lokalizasyonunda somatostatin reseptör görüntüleme başta olmak üzere fonksiyonel görüntüleme yöntemleri önemli bir rol oynamaktadır. Tümör kaynaklı osteomalazi olgusunda, tümör lokalizasyonunu belirlemek amacıyla kullanılan galyum-68 ( $^{68}\text{Ga}$ )-DOTATATE,  $^{68}\text{Ga}$ -fibroblast ve  $^{18}\text{F}$ -florodeoksiglukoz pozitron emisyon tomografisi görüntüleme yöntemlerinin bulgularını sunduk.

**Anahtar Kelimeler:** Tümör kaynaklı osteomalazi, fosfatürük mezenkimal tümörler,  $^{68}\text{Ga}$ -DOTATATE PET/BT,  $^{68}\text{Ga}$ -FAPI PET/BT,  $^{18}\text{F}$ -FDG PET/BT

**Address for Correspondence:** Zehranur Tosunoğlu, University of Health Sciences Türkiye, İstanbul Training and Research Hospital, Clinic of Nuclear Medicine, İstanbul, Türkiye

**E-mail:** zehranurtosunoglu@gmail.com **ORCID ID:** orcid.org/0000-0002-8509-1583

**Received:** 02.01.2026 **Accepted:** 01.03.2026 **Epub:** 23.03.2026

**Cite this article as:** Tosunoğlu Z, Soyaltın UE, Öztürk İ, Kaya M, Akkaş BE, Arslan E. Multimodal functional imaging in tumor-induced osteomalacia:  $^{68}\text{Ga}$ -DOTATATE,  $^{18}\text{F}$ -FDG, and  $^{68}\text{Ga}$ -FAPI PET/CT findings. Mol Imaging Radionucl Ther. [Epub Ahead of Print]



Copyright© 2026 The Author(s). Published by Galenos Publishing House on behalf of the Turkish Society of Nuclear Medicine. This is an open access article under the Creative Commons Attribution-NonCommercial-NoDerivatives 4.0 (CC BY-NC-ND) International License.

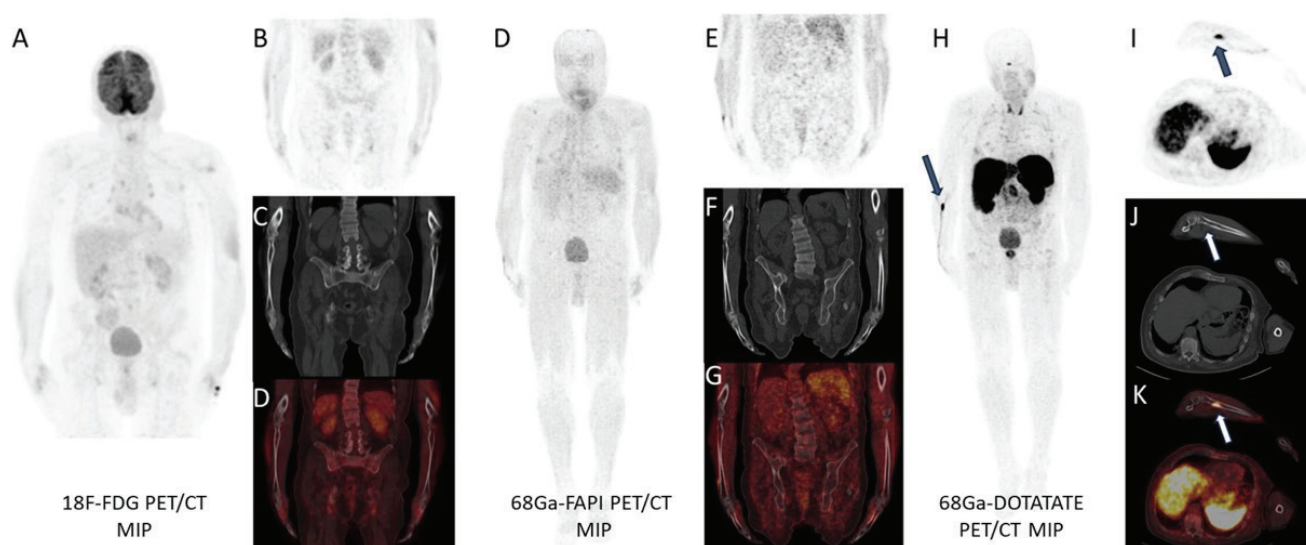


**Figure 1.** A 65-year-old man with a history of bilateral hip fractures treated with prosthetic hip replacements presented with diffuse bodily pain and muscle weakness. The man, who was ambulatory with the aid of a cane, had chronic hypophosphatemia. Laboratory tests revealed a serum phosphate level of 0.8 mg/dL (reference range: 2.5-4.5 mg/dL), a parathyroid hormone level of 70 pg/mL (reference range: 15-65 pg/mL), and a calcitriol (1.25-dihydroxy vitamin D) level of 23 pg/mL (reference range: 20-80 pg/mL). Serum FGF23 levels were elevated. Urinary phosphate excretion was also elevated (1960 mg/day; reference: 400-1300 mg/day). Assessment of bone mineral density by dual-energy X-ray absorptiometry showed T-scores of -1.4 in the lumbar spine and -1.6 in the hip region. Genetic analysis revealed a heterozygous mutation in the *FGF23* gene. With the patient's consent,  $^{18}\text{F}$ -fluorodeoxyglucose positron emission tomography/computed tomography ( $^{18}\text{F}$ -FDG PET/CT) and  $^{68}\text{Ga}$ -fibroblast ( $^{68}\text{Ga}$ -FAPI) PET/CT imaging were performed to determine lesion localization; however, no abnormal tracer uptake was observed (A, D). Subsequently, a  $^{68}\text{Ga}$ -DOTATATE PET/CT scan was conducted. Axial PET and fused PET/CT images (I, K) revealed a focal tracer-avid lesion measuring approximately  $2.5 \times 1.2$  cm at the proximal end of the right radius (maximum standard uptake value: 39.9). Corresponding CT images (J) revealed a mild increase in density within the medullary bone marrow area. The maximum intensity projection image (H) confirmed the localization of the primary lesion in the proximal right radius. Contrast-enhanced magnetic resonance imaging of the right forearm showed a lesion corresponding to the area of  $^{68}\text{Ga}$ -DOTATATE uptake that appeared hyperintense on T2-weighted images, hypointense on T1-weighted images, and exhibited homogeneous contrast enhancement. The patient with additional comorbidities did not consent to histopathological examination. The patient is currently under follow-up and receiving vitamin D and oral phosphate supplementation.

Tumor-induced osteomalacia (TIO) typically originates from phosphaturic mesenchymal tumors, which are usually small, slow-growing, and benign, and can be located in soft tissue or bone throughout the body from the skull to the feet (1,2). These tumors are most commonly localized in the lower extremities and the head and neck region, whereas the upper extremities are the least frequently affected sites (3). Due to their typically small and solitary nature, identifying the exact location of these tumors is often challenging (4). Localization generally begins with functional imaging techniques, including somatostatin receptor (SSTR) imaging ( $^{68}\text{Ga}$ -DOTATATE or octreotide scan) and  $^{18}\text{F}$ -FDG PET/CT (5). In a recent meta-analysis, SSTR-PET/CT demonstrated a higher detection rate for culprit tumors in TIO patients compared to  $^{18}\text{F}$ -FDG PET/CT (6). Fibroblast activation protein inhibitor (FAPI) is known to accumulate in various benign and malignant conditions (7,8). Although only a limited number of TIO cases have been evaluated with FAPI imaging in the literature, some of these have shown uptake at the tumor site (9). We evaluated the contribution of  $^{68}\text{Ga}$ -FAPI PET/CT, alongside  $^{68}\text{Ga}$ -DOTATATE PET/CT and  $^{18}\text{F}$ -FDG PET/CT, to tumor localization in a man with TIO. Our findings demonstrate the superiority of  $^{68}\text{Ga}$ -DOTATATE PET/CT over  $^{18}\text{F}$ -FDG and  $^{68}\text{Ga}$ -FAPI PET/CT for lesion localization.

## Ethics

**Informed Consent:** Written informed consent was obtained from all patients before imaging.

## Footnotes

### Authorship Contributions

Concept: Z.T., U.E.S., İ.Ö., M.Y., B.E.A., Design: U.E.S., İ.Ö., M.Y., B.E.A., E.A., Data Collection or Processing: U.E.S., İ.Ö., M.Y., B.E.A., E.A., Analysis or Interpretation: U.E.S., İ.Ö., M.Y., B.E.A., E.A., Literature Search: U.E.S., İ.Ö., M.Y., B.E.A., E.A., Writing: Z.T., U.E.S., E.A.

**Conflict of Interest:** No conflicts of interest were declared by the authors.

**Financial Disclosure:** The authors declare that this study has received no financial support.

## References

1. Florenzano P, Hartley IR, Jimenez M, et al. Tumor-induced osteomalacia. *Calcif Tissue Int.* 2021;108:128-142.
2. Hautmann AH, Hautmann MG, Kölbl O, et al. Tumor-induced osteomalacia: an up-to-date review. *Curr Rheumatol Rep.* 2015;17:512.
3. Bosman A, Palermo A, Vanderhulst J, et al. Tumor-induced osteomalacia: a systematic clinical review of 895 cases. *Calcif Tissue Int.* 2022;111:367-379.
4. Rayamajhi SJ, Yeh R, Wong T, et al. Tumor-induced osteomalacia - current imaging modalities and a systematic approach for tumor localization. *Clin Imaging.* 2019;56:114-123.
5. Jan de Beur SM, Minisola S, Xia WB, et al. Global guidance for the recognition, diagnosis, and management of tumor-induced osteomalacia. *J Intern Med.* 2023;293:309-328.
6. Meyer M, Nicod Lalonde M, Testart N, et al. Detection rate of culprit tumors causing osteomalacia using somatostatin receptor PET/CT: systematic review and meta-analysis. *Diagnostics (Basel).* 2019;10:2. Published 2019 Dec 18.
7. Tosunoğlu Z, Bozkurt M, Erdamar S, et al. Inflammatory <sup>68</sup>Ga FAPI-46 uptake mimicking a sister Mary Joseph's nodule in a case of gastric signet ring cell carcinoma. *Clin Nucl Med.* Published online May 14, 2025.
8. Şahin ÖF, Alçın G, Ergül N, Çermik TF, Arslan E. Physiological gallbladder accumulation on <sup>68</sup>Ga-FAPI-46 PET/CT. *Clin Nucl Med.* 2024;49:e685-e686.
9. Raeisi N, Saber Tanha A, Mosavi Z, et al. Phosphaturic mesenchymal tumor in the foot detected by <sup>99m</sup>Tc-FAPI-46 SPECT/CT and <sup>18</sup>F-FDG PET/CT. *Clin Nucl Med.* Published online June 4, 2025.